


# Learning from Synthetic Models of Extracellular Matrix; Differential Binding of Wild Type and Amyloidogenic Human Apolipoprotein A-I to Hydrogels Formed from Molecules Having Charges Similar to Those Found in Natural GAGs

Silvana A. Rosú<sup>1,2</sup> · Leandro Toledo<sup>3</sup> · Bruno F. Urbano<sup>3</sup> · Susana A. Sanchez<sup>3</sup> · Graciela C. Calabrese<sup>4</sup> · M. Alejandra Tricerri<sup>1,2</sup> 

Published online: 20 June 2017  
© Springer Science+Business Media, LLC 2017

**Abstract** Among other components of the extracellular matrix (ECM), glycoproteins and glycosaminoglycans (GAGs) have been strongly associated to the retention or misfolding of different proteins inducing the formation of deposits in amyloid diseases. The composition of these molecules is highly diverse and a key issue seems to be the equilibrium between physiological and pathological events. In order to have a model in which the composition of the matrix could be finely controlled, we designed and synthesized crosslinked hydrophilic polymers, the so-called hydrogels varying the amounts of negative charges and hydroxyl groups that are prevalent in GAGs. We checked and compared by fluorescence techniques the binding of human apolipoprotein A-I and a natural mutant involved in amyloidosis to the hydrogel scaffolds. Our results indicate that both proteins are highly retained as long as the negative charge increases, and in addition it was shown that the mutant is more retained than the Wt, indicating that the retention of specific proteins in the ECM could be part of the pathogenicity. These results show the importance of the use of these polymers as a model to get deep insight into the studies of proteins within macromolecules.

**Keywords** Amyloidosis · Human apolipoprotein A-I · Synthetic hydrogels · Extracellular matrix

## Abbreviations

apoA-I	Apolipoprotein A-I
DNCl	Dansyl chloride
ECM	Extracellular matrix
FITC	Fluorescein isothiocyanate
GAGs	Glycosamine glycans
GndHCl	Guanidine hydrochloride
HEMA	2-Hydroxyethyl methacrylate
HDL	High density lipoproteins
LDL	Low-density lipoprotein
PGs	Proteoglycans
SSNa	Sodium 4-styrene sulfonate
ThT	Thioflavin T

## 1 Introduction

Specific interactions among apolipoproteins and components of the extracellular matrix (ECM) particularly proteoglycans (PGs) seem to be clue to regulate events associated to atherosclerosis. Moreover, the different glycosamine glycans (GAGs) have been reported to change in extent, the position of sulfate substitution and composition depending on age, differentiation state, and pathological conditions [1]. In this trend, it was observed that the biglycan (a small leucine-rich repeat PG) and versican (a large chondroitin sulfate PG) were present in atherosclerotic intima, very often with distinctly different distributions [2]. The pathological landscape showed to be very specific, biglycan frequently colocalized with apolipoproteins apoE, apoA-I, and apoB in locations where versican is absent [3].

✉ M. Alejandra Tricerri  
aletricerri@yahoo.com

<sup>1</sup> Instituto de Investigaciones Bioquímicas de La Plata (INIBIOLP), CONICET, La Plata, Buenos Aires, Argentina

<sup>2</sup> Facultad de Ciencias Médicas, Universidad Nacional de La Plata, Calle 60 y 120 S/N La Plata, 1900, La Plata, Buenos Aires, Argentina

<sup>3</sup> Departamento de Polímeros, Facultad de Ciencias Químicas, Universidad de Concepción, Concepción, Chile

<sup>4</sup> Cátedra de Biología Celular y Molecular, Facultad de Farmacia y Bioquímica, Universidad de Buenos Aires, Junín 954, Primer Piso, C1113AAD Buenos Aires, Argentina

The fine equilibrium of the interactions between apolipoproteins and the endothelium is altered in the genesis of atherosclerosis. The binding of oxidized low-density lipoprotein (LDL) to the biglycan, present in the ECM, may favor its retention and subsequent phagocytosis by macrophages in the intima. On the other hand, the high density lipoproteins (HDL) and their main protein apoA-I are proposed to inhibit this process, protecting the intima against foam cells accumulation and plaque formation [4].

The composition and structure of PGs is highly heterogeneous *in vivo*. These charged molecules play key roles within different compartments including cellular surface, ECM, or in the cytoplasm. Both, the polysaccharide chains (GAGs) or the proteins to which they bind confer a large variety of properties and functions [5]. Several PGs have been described, and they differentiate from each other by the nature of the GAGs bound to the core proteins. Although GAGs are long and unbranched polysaccharide chains rich in negative charges due to their carboxylated or sulfated sugar residues, the length, charge distribution and composition seem to be the clue to participate in well controlled functions such as metabolites transport, growth factors receptors, and lipoproteins binding [6, 7].

Amyloidosis constitutes a heterogeneous group of diseases involving protein misfolding and deposition as insoluble fibrils. The natural tendency of the proteins to aggregate could be elicited either by specific pathological cellular micro environments or due to single point hereditary mutations. Many unrelated proteins have been implicated in amyloidosis, including amyloid A protein, islet amyloid polypeptide (IAPP, also known as amylin), prion protein, transthyretin, synuclein, A $\beta$  peptide, light chains of immunoglobulins, apolipoprotein A-I, etc. [8].

In spite of the huge body of research stating the role in amyloidosis, the precise mechanism by which GAGs induce aggregation-prone protein conformations is far from elucidation. While interaction with heparin sulfate has been identified as stabilizing amyloid fibers from different proteins [9], low molecular weight heparins (LMWH) have been suggested as inhibitors of such effect [5]. The intimate association between amyloid deposits and the ECM was elegantly demonstrated in amyloidosis-induced animal models. Shortening of heparan sulfate chains by heparanase over expression resulted in a decrease of amyloid deposition in tissues from mice in an inflammation-associated serum amyloid A amyloidosis [10]. In addition, following decellularization, the liver of transgenic mice over expressing serum amyloid protein showed a marked modification of the normal structure of the ECM, which was overlaid with amyloid deposits [11]. Moreover, the accumulation of the PG decorin in kidney amyloid but not in other renal fibrosing disease supports the importance of the ECM composition in this pathology [12].

About 80% of the protein composition of the HDL is represented by apolipoprotein A-I (apoA-I), which highly flexible structure allows its efficient participation in the reverse cholesterol transport. This lipid efflux pathway involves its circulation partially as a lipid-free conformation. But, on the other hand, the native protein structural disorder elicits its propensity to suffer misfolding or aggregation, and thus some natural variants were described inducing amyloidosis, affecting organs in patients with variable severity depending on the mutation present. Moreover, amyloidosis due to the protein with the native sequence has been described as diffuse protein aggregates in atherosclerotic plaques [13]. Although the reason why this protein is associated to the pathology is still unknown, we have suggested that specific interactions of apoA-I with GAGs of the ECM could elicit its retention and/or aggregation. In this respect, we have previously tested *in vitro* the binding of wild type apoA-I (Wt apoA-I) and the pro-amyloidogenic mutant Arg173Pro to heparin (used as a model of GAG). We showed that formation of amyloid-like complexes between Wt apoA-I and heparin increased under acidic conditions [14]. In addition, Arg173Pro forms heparin-protein complexes at pH 7.4 with higher efficiency than Wt [15]. Thus, it is clear that mild charge content or structural modifications is an important parameter in the regulation of protein–GAGs binding and consequently in protein function. The fact that Arg173Pro, at physiological pH, binds to stronger affinity than the Wt poses the question on the reason for the organ specificity of mutant's deposits: Could the specific retention of proteins within the ECM induce structural changes and pathological rearrangements of these macromolecules?

To study the effect of the ECM in the aggregation state of a protein is important to find a model where the composition of the matrix could be finely controlled. The design of crosslinked hydrophilic polymers, so-called hydrogels, is an important development in the biomedical field as they can mimic, due to their hydrated and porous structure, the micro-environment in which cells are supported in their native landscape [16, 17]. Hence, the construction of synthetic hydrogels offers the possibility of building model matrices where composition could be closely controlled. Sulfate residues and hydroxyl groups are components of most GAGs and they are present in several precursor compounds used to synthesize hydrogels, for example—styrene sulfonic acid and 2-hydroxyethyl methacrylate monomers, hence they were chosen to obtain hydrogels for testing protein binding and retention within the polymer scaffold.

## 2 Materials and Methods

### 2.1 Materials

Guanidine hydrochloride (GndHCl) and thioflavin T (ThT), heparin sodium salt (H-3149), heparin ammonium salt (H-0880) and low molecular weight heparin [H-3400] were from Sigma-Aldrich (St. Louis, USA). His-purifying resin was from Novagen (Darmstadt, Germany). Heparin (for clinical application) from bovine intestinal mucosa (molecular weight 15 kDa) was from Rivero (BA, Argentina); 4,4'-dianilino-1,1'-binaphthyl-5,5'-disulfonic acid, dipotassium salt (Bis-ANS), dansyl chloride and fluorescein isothiocyanate (FITC) were purchased from molecular probes (Invitrogen, Carlsbad, CA). For the hydrogel synthesis the reagents sodium 4-styrene sulfonate (SSNa) and 2-hydroxyethyl methacrylate (HEMA, 97%), ammonium persulfate (APS, 98%), and *N,N*-methylene-bis-acrylamide (MBA, 99%) were purchased from Sigma-Aldrich, while *N,N,N,N'*-tetramethylethylenediamine (TEMED, 99%) were obtained from Merck Co. All other reagents were of the highest analytical grade available.

### 2.2 Methods

#### 2.2.1 ApoA-I Isolation and Purification

Wild type apoA-I (Wt) and the amyloidogenic mutant Arg173Pro were obtained by traditional Molecular Biology techniques and purified as previously described [15]. Purification was checked and confirmed by polyacrylamide gel electrophoresis as stained with Coomassie Blue. In order to ensure freshly monomeric folding of the proteins, the variants were solubilized before each experiment into 2 M GndHCl and exhaustively dialyzed against the chosen buffers.

#### 2.2.2 Labeling of apoA-I with Fluorescence Probes

Dansyl chloride (DNCl) covalently binds to proteins in the amine residues. The probe was solubilized in cold acetone and added to apoA-I in phosphate buffer pH 8.0 at a molar ratio about 10:1 probe:protein. Following overnight incubation while stirring at 4 °C, unbound probe was removed by elution through NAP five columns (GE Healthcare Bio-Sciences, PA). Protein was quantified by the colorimetric Bradford assay, and binding efficiency was calculated to be about four probe molecules per protein by using DNCl extinction coefficient at 340 nm ( $4300 \text{ M}^{-1} \text{ cm}^{-1}$ ). In a similar manner, proteins were labeled with FITC. Briefly, proteins (Wt and Arg173Pro) were taken to phosphate buffer at pH 9.0, and FITC was added in small aliquots from a stock solution in the same buffer. Efficiency was calculated from

the extinction coefficients at 492 nm ( $75,000 \text{ M}^{-1} \text{ cm}^{-1}$ ) being similar for both proteins and around five moles FITC per mole of protein. In order to confirm that the labeling procedure does not induce a sensitive conformational shift in protein structure, Wt (either unlabeled or DNCl-Wt) were set at 0.1 mg/mL and titrated with GndHCl. The shift in the intrinsic fluorescence of the native Trp residues (in positions 8, 50, 72, and 104) was followed as previously reported to determine the chemical stability and denaturation pattern.

#### 2.2.3 Construction of Polymeric Matrices

To design the synthetic polymeric matrices, monomers were chosen with ionic and non-ionic polar groups that could mimic those present in the natural GAGs: sodium 4-styrene sulfonate (SSNa) and 2-hydroxyethyl methacrylate (HEMA). Two copolymers with different SSNa:HEMA mole ratios were synthesized 0.75 and 0.25, maintaining a total monomer concentration of 1.25 mol/L. The synthesis was performed through radical polymerization, by using the crosslinker *N,N*-methylene-bis-acrylamide (5.0 mol%), and ammonium persulfate (APS, 0.5 mol%) and *N,N,N,N'*-tetramethylethylenediamine (TEMED 1.0 mol%), as initiator and co-initiator, respectively; the mol% were calculated based on the sum of monomers used in the feed (Fig. 1). To obtain a gel phase, a dissolution containing the monomer, initiators, and crosslinker was spread into appropriate flat surface containers and incubated at 60 °C for polymerization. The gel point was achieved after 2 h. To analyze the matrices topology, a specimen of the hydrogels was analyzed by scanning electron microscopy.

#### 2.2.4 Incubation of apoA-I Variants with Matrices

In order to analyze whether there is a differential binding of Wt to matrices with different charge (and relative amounts of sulfate groups), apoA-I labeled with DNCl (DNCl-Wt) was incubated with matrices containing SSNa/HEMA at the molar ratios 0.75 or 0.25. A piece of 0.05 g of each matrix was incubated with labeled protein (final concentration 3.6  $\mu\text{M}$  at 37 °C for 24 h) with mild agitation (400 rpm). Afterwards, samples were spun at 12,000 rpm for 20 min; supernatant (100  $\mu\text{L}$ ) was separated and the same volume of Tris buffer added to the matrix. Fluorescence was read in a Beckman DTX 880 Microplate Reader with excitation and emission filters centered at 360 and 535 nm, respectively. In addition, and in order to compare the binding affinity of the mutant Arg173Pro with respect to Wt, we incubated DNCl-Wt and DNCl-Arg173Pro with 0.75 matrix and analyzed the binding with the same methodology.

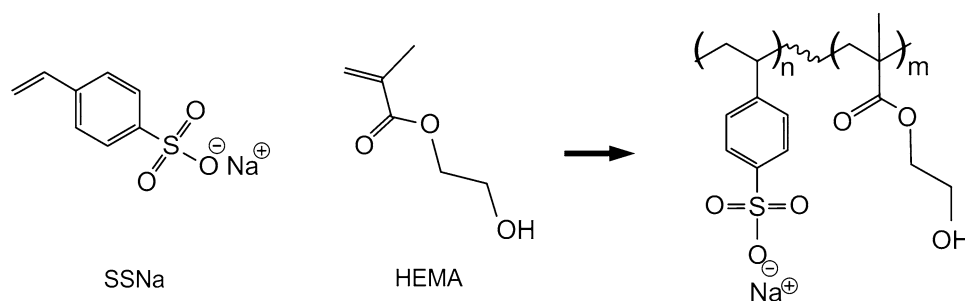


**Fig. 1** Scheme of the synthesis of copolymer P (SSNa-co-HEMA). Monomers [sodium 4-styrene sulfonate (SSNa) and 2-hydroxyethyl methacrylate (HEMA)] were incubated at different molar ratios (pH 7.0) with APS and matrices polymerized following incubation at

60°C in the presence of the initiator and co-initiator. The gel point was achieved after 2 h. By incubating different molar ratios of monomers in the mixture, the number of SSNa (*n*) or HEMA (*m*) monomers incorporated the matrix can be modified

In a different setup square pieces of similar size and same weight of both matrices were incubated with FITC-labeled apoA-I variants (final concentration 1.1 μM) in Tris 20 mM pH 7.4 buffer at 37°C for 24 h. Protein remaining in the surface was washed three times with Tris buffer and samples were observed under a confocal spectral microscope [Centro de Microscopía Avanzada (CMA), Bío-Bío, Universidad de Concepción, Chile]. A z-stack of 100 images was taken from same areas of the gels and the full 3D reconstruction was obtained using the Image-J software. Using the same program the fluorescence intensity from the 100 images was calculated for each matrix, keeping the laser power and all the microscope acquisition parameters constant.

### 2.2.5 Interaction of Proteins with Polymer Scaffolds

We set up to determine whether a sensitive conformational shift or aggregation of the proteins could occur by the interaction with the synthetic matrices. Arg173Pro (at a final concentration of 0.2 mg/mL) was incubated for 24 h at 37°C with an excess amount (0.5 mM) of HEMA or SSNa. Protein structure was characterized as previously described [15, 18]. Intrinsic Trp fluorescence was measured by exciting at 295 nm and registering emission between 310 and 400 nm. Measurements were performed on an Olis upgraded SLM4800 spectrofluorometer (ISS Inc, Champaign, IL). Hydrophobic pockets were estimated by the Bis-ANS probe [19]. Protein was incubated under the same conditions and Bis-ANS was then added at a 1:1 molar ratio (probe:protein). Fluorescence emission was measured by exciting at 395 nm and emission registered between 450 and 550 nm, respectively. To detect amyloid-like aggregation, the protein was incubated at 0.2 mg/mL under the same conditions and after 24 h, thioflavin T (ThT) was added at a 1:1 molar ratio; fluorescence intensity was measured on the Microplate Reader, using excitation and emission filters centered at 430 and 480 nm, respectively.

The interaction of Arg173Pro with ligands was analyzed by native polyacrylamide gradient gel electrophoresis (PAGE). Protein at 0.2 mg/mL was incubated with ammonium or sodium unfractionated heparins (UFH) or low molecular weight heparin (LMWH) at molar a ratio 1:1 protein to heparin for 24 h at 37°C. In a different experiment, Arg173Pro, was incubated with heparin at pH 7.4 either in the presence or absence of 0.5 mM of HEMA or SSNa monomers. The complex migration was visualized by silver stain.

## 3 Results

Polymer scaffolds were synthesized through radical polymerization varying the mole ratio of sodium 4-styrene sulfonate (SSNa) and 2-hydroxyethyl methacrylate (HEMA) with the aim to obtain hydrogels with different amount of negative charge moieties (Fig. 1). Two copolymers with different SSNa:HEMA mole ratios (0.75 and 0.25) were synthesized, maintaining a total monomer concentration of 1.25 M. The nomenclature used to name the polymers corresponds to the fraction of SSNa, being 0.75 or 0.25. Since SSNa comes from a strong acid, then its conjugated base exhibits a less dependence of the pH.

Scanning electron microscopy was used to compare the influence of the sulfonate or hydroxyl groups on the hydrogels topology (Fig. 2). Gels containing lower amount of SSNa in the feed (matrix 0.25) (i.e., lower concentration of negative charge in the polymer) show a smoother surface with pores of different diameters (Fig. 2a, b). Instead, the enrichment in SSNa molar ratio with respect of HEMA (matrix 0.75) results in a spiky surface with more regular topology (Fig. 2c, d).

The differential binding of apoA-I to the matrices having different ratios of SSNa to HEMA was determined using fluorescently labeled apoA-I variants. First, we set out to analyze the effect of the labeling on protein structure by



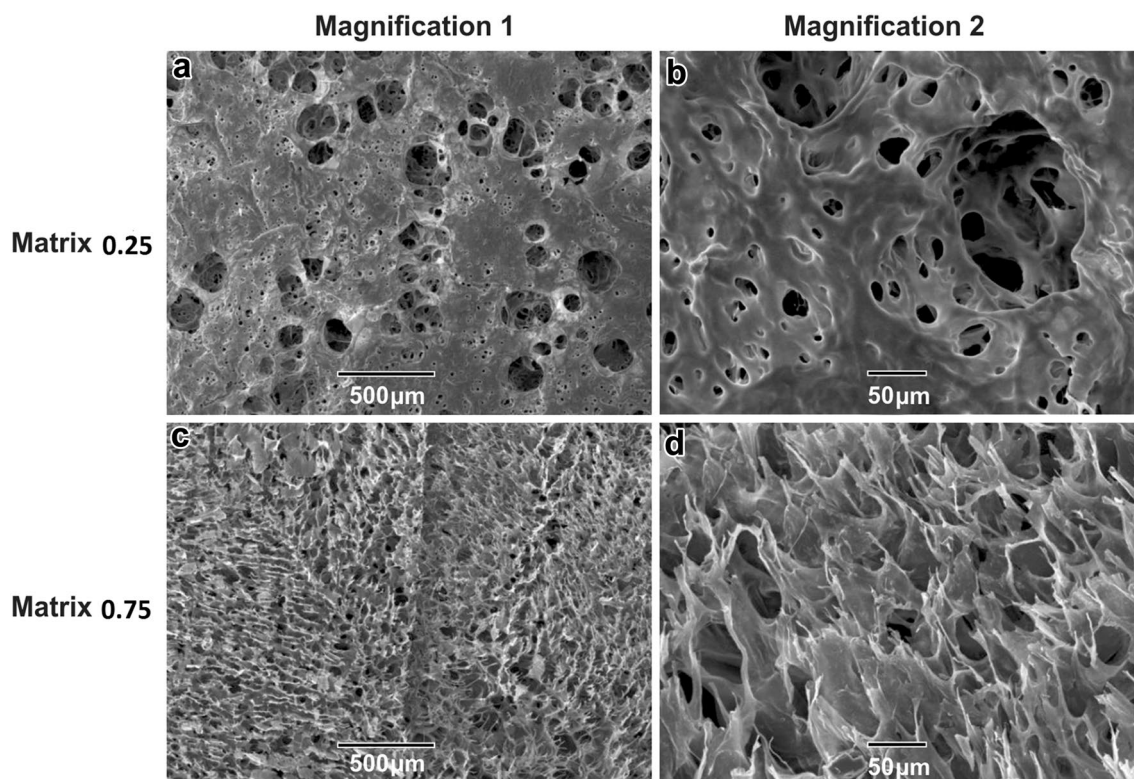


**Fig. 2** Scanning electron microscopy images of the copolymer. Copolymers P (SSNa-co-HEMA) containing 0.25 (a, b) and 0.75 SSNa (c, d) fractions were analyzed by SEM under different magnifications. Bars in the images show the scale used in each case

following the well-known denaturation pattern by Gnd-HCl. Figure 3a shows that the shift in the center of mass of the Trp residues of the Wt protein (dark circles) follows a two-state, cooperative denaturation pattern as described in numerous reports [14]. The fact that this behavior was almost indistinguishable from the DNCI-labeled protein (Fig. 3a, empty circles) indicates that protein conformation is preserved. The DNCI-labeled Wt was incubated with the matrices and the amount of protein bound was determined by quantifying the fluorescence associated to the matrix and to the supernatant after centrifugation to separate the unbound protein. Figure 3b shows that about 42% of the protein remained associated to the 0.75 matrix, while only 19% appeared bound in the 0.25. Arg173Pro, a mutant of apoA-I where a positive amino acid (arginine) in position 173 is replaced by a proline was reported to be present in amyloid deposits especially in heart tissue of patients [20]. In a parallel experiment we checked the interaction of DNCI-Arg173Pro with the 0.75 matrix, showing the same behavior than Wt. In addition a slight by significant binding is observed in this case (inset in Fig. 3b).

As labeling occurs in the amine groups, we checked whether dansylation could modify the binding of the protein to the matrices. Thus, we incubated the same amounts of labeled or unlabeled Wt with the 0.75 matrix for 24 h at

37 °C. Supernatant was then separated and protein remaining in both fractions quantified. We concluded that labeling did not interfere with protein interaction to the hydrogel, as the same amount of Wt or DNCI-Wt was bound (not shown). In addition, we checked the pH of the matrices, as protein conformation could depend on the acidic condition of the media. Both 0.75 and 0.25 matrices showed a pH close to 6.0. Thus, as we have previously reported that protein conformation is preserved under this condition [15], we assumed no influence of pH in the different tested conditions.

In a different set up, and in order to further confirm the previous result, we labeled both Wt and Arg173Pro with FITC and incubated with the matrices overnight. The intensity of the labeled protein bound to the matrix was registered in a confocal microscope. For comparison purposes, the same areas, acquisition parameters and constant pH were maintained. Several *z* planes were acquired and a 3D reconstruction was obtained (Fig. 4a). Using Image J software, the total fluorescence intensity from the proteins was calculated by integrating the intensity per plane (Fig. 4b). Control experiments using matrices incubated without the labeled proteins showed no signal in the emission range used to observe the FITC labeled apoA-I. In agreement with the cuvette experiment

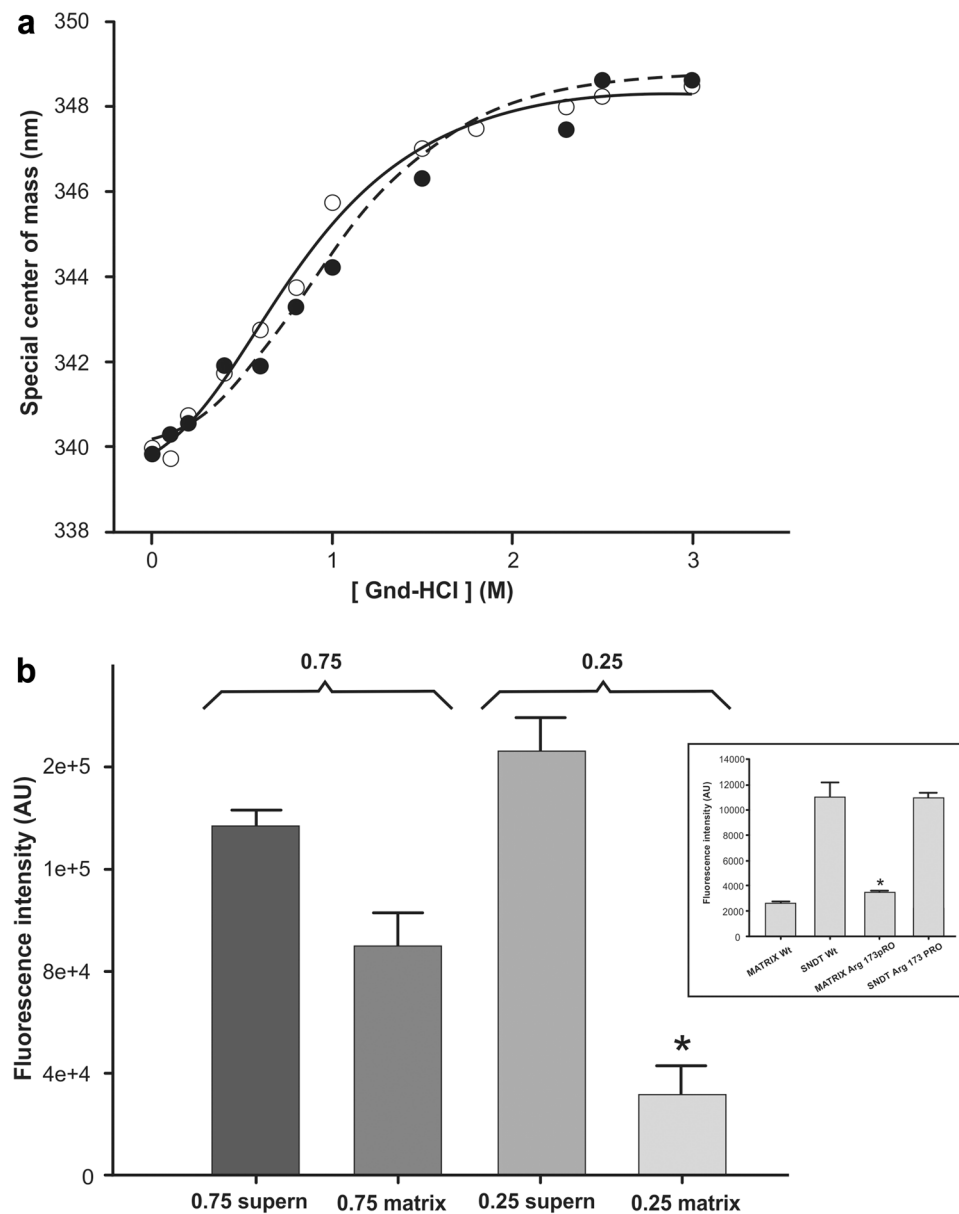


**Fig. 3** Quantification of the binding of DNCl labeled wt apoA-I to matrices. **a** Effect of labeling on protein conformation followed by chemical denaturation. The Wt protein either labeled with DNCl (*empty circles*) or unlabeled (*dark circles*) was set to 0.1 mg/mL in citrates phosphates Mc Ilvaine's buffer, pH 7.4 and titrated with increasing concentrations of GndHCl. Trp fluorescence emission spectra were obtained by excitation at 295 nm, and scanning the emission between 310 and 420 nm. With these data, the center of mass was calculated for each sample. **b** 0.05 g of the different matrices were incubated with DNCl-Wt. Supernatant (*supern*) was separated and matrix taken to the original volume with buffer. Each one

of both fractions was set in an optical dark fluorescence multiplate, and DNCl-associated fluorescence measured [represented as arbitrary units (AU)] with excitation and emission filters of 360 and 535 nm respectively. *Bars* correspond to means  $\pm$  SE. \*Difference on the protein remaining in the matrix (0.25) respect to the protein bound to matrix 0.75 at  $p < 0.05$ . Results are representative of three experiments under the same conditions. *Inset* Wt and Arg173Pro were incubated with the 0.75 matrix and bound proteins analyzed under the same conditions than in Fig. 3b. \*Difference on the Arg173Pro remaining in the matrix respect to Wt at  $p < 0.01$

(Fig. 3b), the total intensity associated to the 0.75 matrix incubated with WT apoA-I is higher than the intensity associated to 0.25. In addition, and interestingly, the intensity associated to both matrices (0.75 and 0.25) was higher when incubated with Arg173Pro.

Finally, we studied the possible structural alterations of Arg173Pro as a consequence of its binding to the monomers that may favor protein retention and/or aggregation. Thus, the protein was incubated with an excess of monomers (either SSNa or HEMA) and biophysical

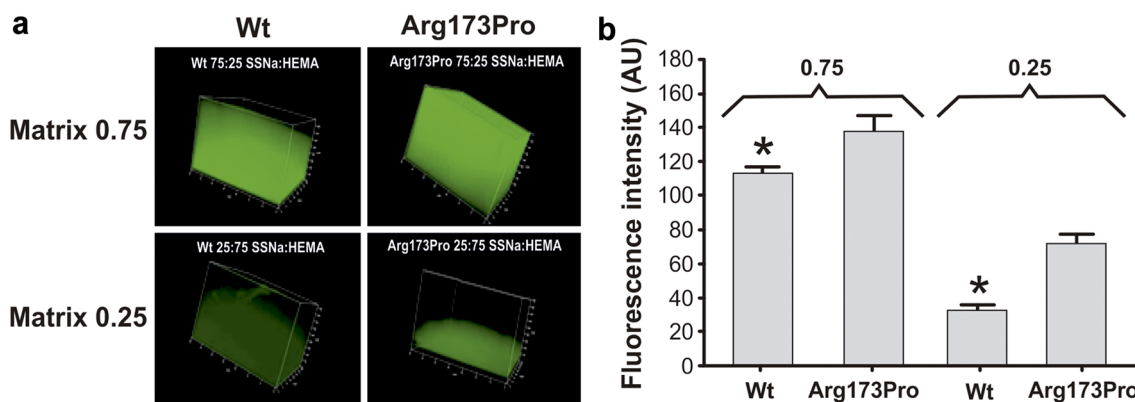


**Fig. 4** Characterization of apoA-I binding to matrices. 3-D images (a) and integrated intensity (b) of FITC-fluorescence associated to hydrogels [represented as fluorescence relative units (RU) obtained by the Image-J software]. Images were taken at room temperature, with excitation at a 488 nm and emission under a 512 m $\pm$ 20 nm. A

stack of 100 images was acquired, every 9  $\mu$ m. Bars correspond to means  $\pm$  SE. \*Difference of the Wt respect to Arg173Pro in the same matrix (either 0.75 or 0.25) at  $p < 0.05$ . Results are representative of three experiments under the same conditions

measurements were used to characterize its structure. Tryptophan emission is characteristic of the secondary structure of a protein and is normally used to detect structural alterations [14]. The tryptophan spectra remained similar in the presence of monomers (not shown). Spatial rearrangement of a protein can be inspected using Bis-ANS [21]. This Fluorescent dye senses the hydrophobic pockets, and the changes in spatial rearrangements are shown in emission spectral shifts and intensity changes [18]. The binding of Bis-ANS to the apoA-I variant was not significantly altered as it cannot be suggested as either a significant intensity or a shift of the center of mass to the spectra detected in the presence of the monomers SSNa or HEMA (Fig. 5a).

The fluorescent dye thioflavin T was used in order to detect whether interaction of the protein with the monomers could induce a misfolded conformation. The strong fluorescence quantum yield of this probe upon binding to pro-amyloid aggregates (but low as free in solution) is well described [22]. When Arg173Pro is incubated at physiological pH, a clear low binding to ThT indicates the tendency of the protein to form structures that could be sensitive to aggregate [15]. This fluorescence did not increase in the presence of monomers neither the size of the product as checked by light scattering (not shown), indicating that the polar groups of the monomers do not elicit the aggregation tendency of this variant (Fig. 5b).

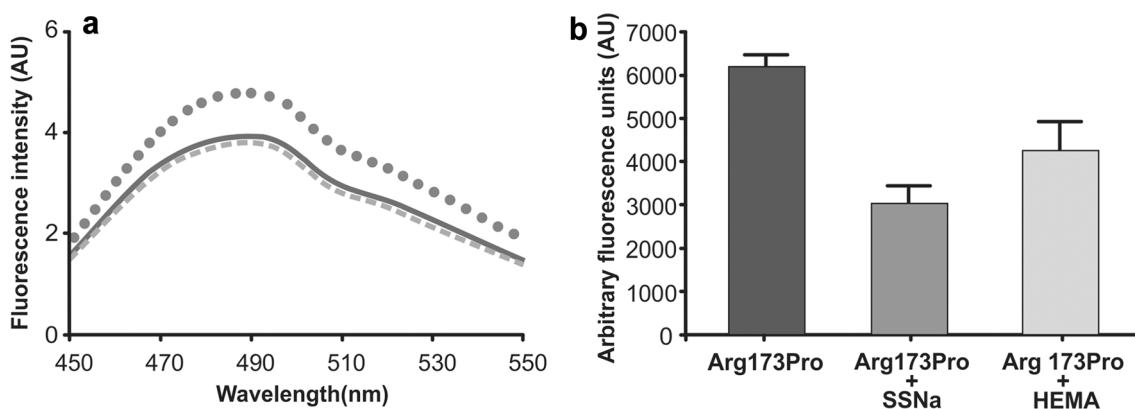


**Fig. 5** Structural characterization of apoA-I variant Arg173Pro upon incubation with HEMA or SSNa monomers. a Arg173Pro (0.2 mg/mL in citrates phosphates McIlvaine's buffer, pH 7.4) was incubated for 48 h at 37°C and Bis-ANS added at a molar ratio 1:1 probe to protein. Spectra were acquired with excitation at 395 and emission registered between 450 and 550 nm; black, dotted and dashed lines

correspond to protein in the absence or the presence of 0.5 mM of HEMA or SSNa, respectively. b Amyloid-like aggregation was detected by the addition ThT to Arg173Pro at a 1:1 molar ratio to protein. Following 48 h incubation at 37°C, fluorescence was quantified in the microplate reader at 480 nm (excitation set at 430 nm). Bars correspond to means  $\pm$  SE

Following, we set out to better characterize the interaction of Arg173Pro with negative charged natural compounds. First, we compared the binding to heparins with different molecular mass at the molar ratio heparin:protein (1:1). Figure 6a shows that, in agreement to our previous results, the incubation of Arg173Pro with either both sodium and ammonium unfractionated heparins (UFH) (lanes 2 and 4 respectively) resulted in an efficient binding as visualized by a shift of the band corresponding to the monomer of apoA-I (28 kDa, lane 1) to a higher molecular size and with fainter intensity. On the other hand, the pattern observed in the gel in the presence of LMWH (lane 3) is indistinguishable in intensity and size with the variant in lane 1, indicating lower or absent interaction of the protein with the GAG.

Therefore, we analyzed whether monomers could compete (and/or inhibit) the binding of Arg173Pro to heparin. In order to test this possibility, we incubated the mutant with heparin and compared its migration on native PAGE electrophoresis in the presence of each monomer. As observed before [15] an efficient protein–heparin binding is detected as the band corresponding to the lipid-free protein (lane 2 in Fig. 6b) vanished, giving rise to bands of larger size corresponding to the protein complexed with the GAG which are not resolved by the gel (lane 3). These structures remained stable even when incubated in the presence of either an excess of SSNa (lane 4) or HEMA (lane 5).

## 4 Discussion

GAGs in the tissues form hydrated gels that fill most of the extracellular space and tend to occupy large volumes even at very low concentrations. These sugars are highly negatively charged macromolecules playing key roles in keeping water, conferring high viscosity to the solution, and participating in weak and specific interactions among different molecules [5]. For instance, two classes of heparin, UFH and LMWH, which only differ in the size of their chains showed different anticoagulant activities. The negatively charged pentasaccharide of UFH interacts with three regions which are brought together in folded antithrombin. Nevertheless, LMWH which contains the essential pentasaccharide to bind antithrombin lacks the required length to bind at the same time thrombin as UFH, and only activated factor X [23, 24].

Moreover, specific interactions of GAGs with proteins seem clue in the genesis of amyloidosis. The density of negative charges in the GAGs (due to sulfate or carboxy groups) may interact in specific conformational arrangements within positive residues in the proteins. In vitro studies have shown that though having similar composition the chondroitin sulfates and heparin sulfate GAGs show different efficiency in the aggregation pathways of amyloid proteins such as the A $\beta$  peptide or immunoglobulin light chains [7, 25–27].

In support to the importance of the specific–electrostatic interactions among GAGs and proteins, small-molecule

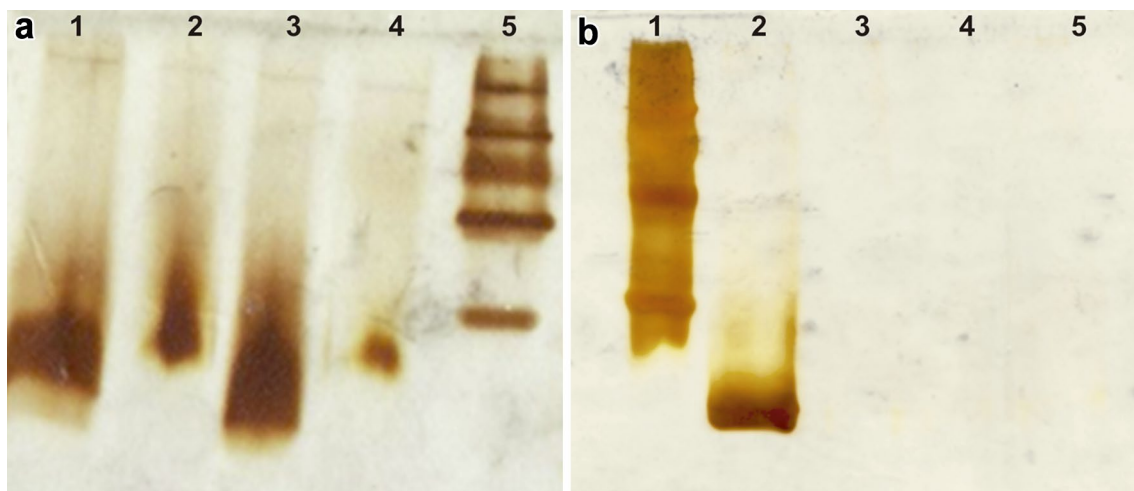


**Fig. 6** Characterization of the binding of Arg173Pro to ligands by electrophoresis. **a** Native PAGE gel 4–25% detected by silver staining. Arg173Pro was incubated as indicated in Sect. 2.2 without (lane 1) or with ammonium unfractionated heparin (UFH) (lane 2), low molecular weight heparin (LMWH) (lane 3) or sodium UFH (lane 4) at molar ratio heparin:protein 1:1 for 24 h at 37 °C. Same amount of Arg173Pro was loaded in each lane. Lane 4 corresponds to high molecular weight standards 669, 440, 232, 140 and 67 kDa (Amer-

sham Biosciences, UK). **b** A similar native PAGE was loaded and detected as in (a) Arg173Pro was incubated in the absence (lane 2) or the presence of heparin at molar ratios heparin:protein 10:1 (lanes 2); Arg173Pro and heparin in the last molar ratio were incubated under the same condition in the presence of 0.5 mM of SSNa (lane 3) or HEMA (lane 4). Same amount of Arg173Pro was loaded in each lane. Lane 1 corresponds to high molecular weight standards as in (a)



anionic sulfonates or sulfates used in pre-clinical studies significantly reduced amyloid progression, indicating that these groups having structural similarities with GAGs' motifs compete with the formation of fibrils aggregates [28].

The results obtained here strongly support that the increase in negative charge of the GAG (in our study the polymer with the highest SSNa content) results in higher protein binding. The fact that the binding of apoA-I Wt to heparin is enhanced at pH lower than the physiological indicates that protonation of the protein amino acids, i.e., histidine, may participate in electrostatic interactions with the negative charges of the GAG [14]. As Arg173Pro (which loses a positive residue) shows stronger binding to this matrix indicated that in addition to the charge, conformation arrangements are key to determine the strength of the interaction. We have previously proposed that the disruption of helix 7 due to the Pro residue allows the exposure of cryptic positive residues (Arg) that could potentially interact with the GAGs [15]. Moreover monomers did not produce a drastic effect on protein conformation or binding to other molecules such as heparin. The decreased efficiency of Arg173Pro-LMWH binding as compared to larger heparins supports in addition a cooperative binding driving this interaction. Thus, the matrix seems to work as a basal "platform" in which charges, viscosity, and probably structural pockets help to the strength of the interaction and protein retention in the microenvironment. Townsend et al. have recently proposed that heparin induces self assembly of the N-terminal domain of the protein which elicits fibril-like conformations [29].

The observed stronger binding of apoA-I variants to the sulfonated-rich matrix supports the fact that (at least for this mutant) part of the pathological mechanism could be due to a higher retention and/or aggregation in the ECM. This induced protein aggregation could, in addition, diminish the physiological amount of protein available to participate in the lipid-removal pathways.

In order to design drugs as therapy to halt the pro-amyloid cascades it is essential to understand the interaction of amyloidogenic proteins with partners in circulation such as GAGs. Based on previous studies, novel negative molecules are being tested in order to inhibit the binding of misfolded proteins to GAGs and thereby these agents could be appropriate to avoid the retention and deposition of fibrillar aggregates in tissues [30]. These studies involve sulfate groups with different efficiency either in vivo or in vitro models, and could be new strategies to inhibit the pathological aggregation of amyloid proteins.

In this trend, it is evident that a fine control of charges or polarity is clue to understand and mediate in the interaction of apoA-I variants within partners of the microenvironment. The polymers herein used are easy to build and

to characterize, reproducible, and their optical properties allow to be studied by fluorescence so as to analyze the binding and the conformation of interacting proteins such as apoA-I and the pathological mutants. Even though we are aware of the chemical complexity of the biological ECM, the construction of polymers with different composition will help us deeply investigate the identity of apoA-I and its variants interactions with partners in the ECM.

**Acknowledgements** Authors acknowledge Mario Ramos for his expertise in Figure preparations, Gabriela S. Finarelli for collaboration with proteins expression and purification and to Rosana del Cid for English assistance. The work presented here was supported by Universidad Nacional de La Plata (Grant Numbers M158 and M187 to M. A. Tricerri), Consejo Nacional de Investigaciones Científicas y Técnicas, Argentina (PIP 112 201101-00648), S. A. Sanchez acknowledges Fondo Nacional de Desarrollo Científico y Tecnológico de Chile (Fondecyt Grant Number 1140454). B. F. Urbano thanks to VRID Enlace 216.024.040-1.0. GC Calabrese acknowledges the financial support of the University of Buenos Aires (Grant# 20020130100626BA).

#### Compliance with Ethical Standards

**Conflict of interest** The authors declare that they have no conflicts of interest.

**Ethical Approval** This article does not contain any studies with human participants or animals performed by any of the authors.

#### References

1. Kinsella MG, Bressler SL, Wight TN (2004) The regulated synthesis of versican, decorin, and biglycan: extracellular matrix proteoglycans that influence cellular phenotype. *Crit Rev Eukaryot Gene Expr* 14:203–234
2. Gutierrez P, O'Brien KD, Ferguson M et al (1997) Differences in the distribution of versican, decorin, and biglycan in atherosclerotic human coronary arteries. *Cardiovasc Pathol* 6:271–278. doi:10.1016/S1054-8807(97)00001-X
3. O'Brien KD, Olin KL, Alpers CE et al (1998) Comparison of apolipoprotein and proteoglycan deposits in human coronary atherosclerotic plaques: colocalization of biglycan with apolipoproteins. *Circulation* 98:519–527. doi:10.1161/01.CIR.98.6.519
4. Calabresi L, Gomaschi M, Franceschini G (2003) Endothelial protection by high-density lipoproteins: from bench to bedside. *Arterioscler Thromb Vasc Biol* 23:1724–1731. doi:10.1161/01.ATV.0000094961.74697.54
5. Iannuzzi C, Irace G, Sirangelo I (2015) The effect of glycosaminoglycans (GAGs) on amyloid aggregation and toxicity. *Molecules* 20:2510–2528. doi:10.3390/molecules20022510
6. Oberkersch R, Maccari F, Bravo AI et al (2014) Atheroprotective remodelling of vascular dermatan sulphate proteoglycans in response to hypercholesterolaemia in a rat model. *Int J Exp Pathol* 95:181–190. doi:10.1111/iep.12072
7. Nishitsuji K, Uchimura K (2017) Sulfated glycosaminoglycans in protein aggregation diseases. *Glycoconj J*. doi:10.1007/s10719-017-9769-4
8. Chiti F, Dobson CM (2006) Protein misfolding, functional amyloid, and human disease. *Annu Rev Biochem* 75:333–366. doi:10.1146/annurev.biochem.75.101304.123901

9. Díaz-Nido J, Wandosell F, Avila J (2002) Glycosaminoglycans and  $\beta$ -amyloid, prion and tau peptides in neurodegenerative diseases. *Peptides* 23:1323–1332. doi:[10.1016/S0196-9781\(02\)00068-2](https://doi.org/10.1016/S0196-9781(02)00068-2)
10. Li J-P, Galvis MLE, Gong F et al (2005) In vivo fragmentation of heparan sulfate by heparanase overexpression renders mice resistant to amyloid protein A amyloidosis. *Proc Natl Acad Sci* 102:6473–6477. doi:[10.1073/pnas.0502287102](https://doi.org/10.1073/pnas.0502287102)
11. Mazza G, Simons JP, Al-Shawi R et al (2016) Amyloid persistence in decellularized liver: biochemical and histopathological characterization. *Amyloid* 23:1–7. doi:[10.3109/13506129.2015.110518](https://doi.org/10.3109/13506129.2015.110518)
12. Stokes MB, Holler S, Cui Y et al (2017) Expression of decorin, biglycan, and collagen type I in human renal fibrosing disease. *Kidney Int* 57:487–498. doi:[10.1046/j.1523-1755.2000.00868.x](https://doi.org/10.1046/j.1523-1755.2000.00868.x)
13. Obici L, Franceschini G, Calabresi L et al (2006) Structure, function and amyloidogenic propensity of apolipoprotein A-I. *Amyloid* 13:191–205. doi:[10.1080/13506120600960288](https://doi.org/10.1080/13506120600960288)
14. Ramella NA, Rimoldi OJ, Prieto ED et al (2011) Human apolipoprotein A-I-derived amyloid: its association with atherosclerosis. *PLoS ONE*. doi:[10.1371/journal.pone.0022532](https://doi.org/10.1371/journal.pone.0022532)
15. Rosú SA, Rimoldi OJ, Prieto ED et al (2015) Amyloidogenic propensity of a natural variant of human apolipoprotein A-I: stability and interaction with ligands. *PLoS ONE* 10:1–17. doi:[10.1371/journal.pone.0124946](https://doi.org/10.1371/journal.pone.0124946)
16. Geckil H, Xu F, Zhang X et al (2010) Engineering hydrogels as extracellular matrix mimics. *Nanomedicine* 5:469–484. doi:[10.2217/nmm.10.12](https://doi.org/10.2217/nmm.10.12)
17. Slaughter BV, Khurshid SS, Fisher OZ (2009) Hydrogels in regenerative medicine. *Adv Mater* 21(32–33):3307–3329. doi:[10.1002/adma.200802106](https://doi.org/10.1002/adma.200802106)
18. Ramella NA, Schinella GR, Ferreira ST et al (2012) Human apolipoprotein A-I natural variants: molecular mechanisms underlying amyloidogenic propensity. *PLoS ONE*. doi:[10.1371/journal.pone.0043755](https://doi.org/10.1371/journal.pone.0043755)
19. Jameson DM (2014) Introduction to fluorescence. CRC Press, Taylor and Francis Group, Boca Ratón
20. Hamidi Asl K, Liepnieks JJ, Nakamura M et al (1999) A novel apolipoprotein A-I variant, Arg173Pro, associated with cardiac and cutaneous amyloidosis. *Biochem Biophys Res Commun* 257:584–588. doi:[10.1006/bbrc.1999.0518](https://doi.org/10.1006/bbrc.1999.0518)
21. Martins SM, Chapeaurouge A, Ferreira ST (2003) Folding intermediates of the prion protein stabilized by hydrostatic pressure and low temperature. *J Biol Chem* 278:50449–50455. doi:[10.1074/jbc.M307354200](https://doi.org/10.1074/jbc.M307354200)
22. LeVine H (1999) Quantification of  $\beta$ -sheet amyloid fibril structures with thioflavin T. *Methods Enzymol* 309:274–284. doi:[10.1016/S0076-6879\(99\)09020-5](https://doi.org/10.1016/S0076-6879(99)09020-5)
23. Calabrese GC, Recondo EF, De Recondo MEF (2002) Antithrombin and first complement protein recognize the same active heparin fraction. *Thromb Res* 105:537–541. doi:[10.1016/S0049-3848\(02\)00062-2](https://doi.org/10.1016/S0049-3848(02)00062-2)
24. Oberkersch R, Attorresi AI, Calabrese GC (2010) Low-molecular-weight heparin inhibition in classical complement activation pathway during pregnancy. *Thromb Res*. doi:[10.1016/j.thromres.2009.11.030](https://doi.org/10.1016/j.thromres.2009.11.030)
25. Ariga T, Miyatake T, Yu RK (2010) Role of proteoglycans and glycosaminoglycans in the pathogenesis of Alzheimer's disease and related disorders: amyloidogenesis and therapeutic strategies—a review. *J Neurosci Res* 88:2303–2315. doi:[10.1002/jnr.22393](https://doi.org/10.1002/jnr.22393)
26. Blancas-Mejia LM, Hammernik J, Marin-Argany M, Ramirez-Alvarado M (2015) Differential effects on light chain amyloid formation depend on mutations and type of glycosaminoglycans. *J Biol Chem* 290:4953–4965. doi:[10.1074/jbc.M114.615401](https://doi.org/10.1074/jbc.M114.615401)
27. Fraser PE, Darabie AA, McLaurin J (2001) Amyloid- $\beta$  interactions with chondroitin sulfate-derived monosaccharides and disaccharides: implications for drug development. *J Biol Chem* 276:6412–6419. doi:[10.1074/jbc.M008128200](https://doi.org/10.1074/jbc.M008128200)
28. Kisilevsky R, Lemieux LJ, Fraser PE et al (1995) Arresting amyloidosis in vivo using small-molecule anionic sulphonates or sulphates: implications for Alzheimer's disease. *Nat Med* 1:143–148. doi:[10.1038/nm0295-143](https://doi.org/10.1038/nm0295-143)
29. Townsend D, Hughes E, Hussain R et al (2017) Heparin and methionine oxidation promote the formation of apolipoprotein A-I amyloid comprising  $\alpha$ -helical and  $\beta$ -sheet structures. *Biochemistry* 56:1632–1644. doi:[10.1021/acs.biochem.6b01120](https://doi.org/10.1021/acs.biochem.6b01120)
30. Rumjon A, Coats T, Javaid MM (2012) Review of eprodisate for the treatment of renal disease in AA amyloidosis. *Int J Nephrol Renovasc Dis* 5:37–43. doi:[10.2147/IJNRD.S19165](https://doi.org/10.2147/IJNRD.S19165)